AIAA AVIATION Forum
12-16 June 2023, San Diego, CA and Online
AIAA AVIATION 2023 Forum

10.2514/6.2023-3832

Subsonic installed jet noise scattering prediction using BEM and an optimized wave-packet model

Giorgio Palma*
Roma Tre University, Department of Civil, Computer Science and Aeronautical Technologies Engineering, Via Vito Volterra, 62, 00146 Rome (Italy)

S. Meloni†
Department of Economics, Engineering, Society and Business Organization, University of Tuscia, 01100 Viterbo,VT, (IT)

Roberto Camussi,‡, Umberto Iemma,§
Roma Tre University, Department of Civil, Computer Science and Aeronautical Technologies Engineering, Via Vito Volterra, 62, 00146 Rome (Italy)

Christophe Bogey ¶
Laboratoire de Mécanique des Fluides et d'Acoustique, LMFA, UMR 5509, 69130 Ecully, France

The propulsion-airframe acoustic interaction is an aspect of growing interest in aircraft noise assessment. The development of low-order models for the jet noise source is vital to address the scattering from the surfaces with computational costs compatible with the conceptual or preliminary design phase when complete computational fluid dynamics simulations are not yet affordable for the effort and time required. In this study, we use a jet-noise wave-packet model capable of modelling both the hydrodynamic and acoustic part of the pressure fluctuations. The model parameters are optimized using near- and far-field information from a large eddy simulation of a free subsonic jet at multiple radial distances. The use of near-field data is based on the observation that the scattering surfaces are typically separated from the jet axis in the radial direction only by a few nozzle diameters. The noise source is then implemented in an in-house open-source Boundary Element Method code (AcouSTO), solving the Kirchhoff-Helmholtz equation to evaluate the scattering and propagation of the pressure perturbation in the far field. The BEM simulations show an increased directivity in the upstream direction for the installed jet, in agreement with the observation presented in the literature.

I. Introduction

Aviation noise has been widely identified as a driver of several negative stress-mediated health effects, from sleep disorders to cardiovascular issues [1, 2], which incidence is increased in the exposed population. The operation and expansion of airports are nowadays limited by strict regulations aiming at controlling and limiting the exposure of the surrounding community to aircraft noise and the number of people affected by it. Forecasts of the (international regulation authorities) ICAO, published in the last report on Global Environment Trends, indicates that this situation is the most likely scenario in the future, at least for most regions of the world.

The research on noise reduction devices is nowadays very active in all the aircraft areas, involving relatively mature technologies for quieter high lift devices [3], chevrons for jet exhaust [4, 5], the evolution of acoustic liners [6–11] for turbofans ducts, and also more innovative treatments with lower Technology Readiness Level [12]. Jet noise has always been a dominant noise source for turbojets and turbofans especially during take-off operations. So far, it has been mainly tackled by reducing jet velocity, increasing the thrust portion provided by the fan, reaching higher bypass ratios, and improving the propulsive system efficiency. This led to engines with larger relative sizes compared to aircraft, which

*Post–Doc Research Fellow, Department of Engineering, giorgio.palma@uniroma3.it
†Assistant Professor, Department of Economics, Engineering, Society and Business Organization, University of Tuscia, 01100 Viterbo,VT, (IT), stefano.meloni@unitus.it
‡Full Professor, Department of Civil, Computer Science and Aeronautical Technologies Engineering, roberto.camussi@uniroma3.it
§Full Professor, Department of Engineering, umberto.iemma@uniroma3.it
¶CNRS Research Scientist; christophe.bogey@ec-lyon.fr. Associate Fellow AIAA.

integration into the airframe is becoming more and more critical, with the nacelle and the jet coming in the extreme proximity of the wing and high-lift devices. The aerodynamic interference between the jet shear layer and the flaps generates sources of noise that can easily dominate the generic free jet noise.

Projecting the research to the mid- and long-term future, groundbreaking solutions are also being developed, aiming at overcoming the saturation trend in noise reduction that characterizes mature technologies. Innovative configurations such as Blended and Hybrid Wing Body (BWB and HWB) aircraft are probably the most promising alternative to the well-known tube-and-wing configuration in terms of aerodynamic efficiency and community noise reduction [13–16]. The most popular interpretation of these innovative configurations involves the upper installation of the propulsion system on top of the large center body surface, offering interesting acoustic shielding capability to be exploited for engine-related community noise reduction [12, 17, 18]. The propulsion-airframe acoustic interaction is an aspect of growing research interest for future aircraft and should be accounted for since the beginning of the design process.

However, the simulation of the scattering and shielding from large surfaces in the audible range of frequencies can be computationally very expensive, requiring accurate solutions up to extremely high Helmholtz number $He = kl$ (where k is the wave-number and l is the characteristic length of the scattering object). The resources required for direct simulation with high-fidelity CFD or CAA methods make them unfeasible for extensive usage in the conceptual design phase and design optimization processes.

There is hence a strong need for low- and mid-fidelity models and solvers able to catch the fundamental feature of installed jet noise, avoiding the solution of the complete set of equations holding the dynamic of the complex fluid structures involved. Adaptive metamodeling techniques have been recently applied to this class of problems [19, 20] to reduce the computational effort required in determining the optimal position of the propulsion system that minimizes the noise directed towards the ground and community. Artificial Neural Networks, trained with experimental data in both near and far field, have been used as a non-linear surrogate model to predict the noise emitted by a single-stream jet in under-expanded conditions [21], showing good agreement for a wide range of Mach number. Other jet noise models used distributions of acoustic monopoles as noise sources. However, it has been demonstrated that such a simple source is not able to satisfactorily capture the jet noise features [22]. In some low-order models, the noise sources of a single circular jet were represented by a set of uncorrelated quadrupoles [23]. However, it was shown that the directivity at shallow angles was not well reproduced [24]. The perspective on jet noise changed when the presence of coherent structures in jets and their importance in the aft-angle radiation for high subsonic and supersonic jets was demonstrated, providing a basis for the introduction of wave-packets as modeling approach [25, 26]. The wave-packet model has been widely used as a low-order model for the jet noise source. In Papamoschou [27], a virtual cylindrical surface hosting the wave-packet is assumed to surround the jet region and radiate the pressure perturbation. The parameters such as envelope amplitude, wavelength, position, and convection velocity were typically estimated from far-field measurements, optimizing their values and maximizing the agreement on experimental data on a training set [22, 28, 29].

A large body of the literature demonstrated that the low-frequency amplification of the jet noise in the classical jet-wing architecture could be ascribed to the scattering of the jet hydrodynamic field [30–32], and the same mechanism will hold for innovative turbofan powered BWB and HWB. The jet-surface interaction is expected to happen at a few nozzle diameters from the jet axis, both for classic and innovative aircraft configurations, implying that the wave-packet should be calibrated with near-field data to maximize its prediction reliability where the scattering takes place. For the prediction of the acoustic scattering and shielding, source models able to capture the near-field characteristics of the impinging jet noise are needed to accurately address the effects of the wing and/or airframe. Recently, Palma *et. al.* [33, 34] followed the approach introduced by Papamoschou [22, 27–29], calibrating the model parameters on near-field large eddy simulations (LES) data of a high-speed subsonic isothermal jet. The mentioned paper presents a multi-Strouhal number analysis optimizing the wave-packet source model separately for each value in the set $St_D = 0.25,\ 0.5,\ 0.75$ and 1 and using pressure data from the numerical database for the dominant axisymmetric azimuthal mode. It has been shown that optimizing the model parameters with pressure data at multiple distances in the near field provides a noise source that also preserves adherence to the reference data for radial positions outside the training set, improving the reliability of its prediction.

This article aims to extend the work started in [33], training the wave-packet model with information from both the near and far fields using the same multi-objective approach. Data from a high-fidelity LES are used in the optimization defining the reference solutions the optimized wave-packet has to reproduce. An extra far-field line is added to improve the fidelity of the prediction of the optimized source far from the jet axis, providing additional information on the radiating acoustic component of the wave-packet; the near-field lines, on the other hand, contain information also on the hydrodynamic part of the acoustic field. Combining the features of the two classes guides the optimization towards a prediction valid in a wider range of distances. The optimized wave-packet is then coupled with a Boundary Element

Method (BEM) solver for jet noise scattering predictions. The aim is to develop an open-source mid-fidelity tool for predicting installed jet noise scattering and shielding effects.

The paper is organized as follows: the wave-packet model and the BEM theory are described in sections II and III, respectively; Results from the optimization and the BEM simulations are reported in section V. Final remarks can be found in section VI.

II. The wave-packet model

A wave-packet model is used as a source for reproducing the noise produced by a subsonic jet. The one here used has been introduced by Morris [35, 36] and by Tam and Burton [37], Crighton and Huerre [38], and Avital *et al.* [39]. It has been developed by Papamoschou [22, 27–29], which derived the formulation adopted in this paper. The model is based on the fundamental assumption stating that the peak noise radiation from the jet in the aft region is related to the large-scale coherent structures in the jet flow that can be modeled as instability waves at its boundary, growing and then decaying along the axial distance [22].

The present formulation introduces a cylindrical virtual surface surrounding the original jet. The surface radiates the pressure perturbation imposed on it, representing and substituting the jet from the acoustic point of view. Applying the wave-packet ansatz, the pressure on the cylindrical surface at r_0 surrounding the jet is prescribed as:

$$p_w(m, r_0, x, \theta, t) = p_0(x) e^{-i\omega t + im\theta}, \tag{1}$$

where m is the azimuthal mode number, x denotes the axial coordinate, θ is the azimuthal angle, $\omega = 2\pi f$ is the pulsation. The wave-packet axial shape $p_0(x)$ is given in the form [22]:

$$p_0(x) = \tanh\left(\frac{(x - x_0)^{p_1}}{b_1^{p_1}}\right)\left[1 - \tanh\left(\frac{(x - x_0)^{p_2}}{b_2^{p_2}}\right)\right] e^{i\alpha(x - x_0)}. \tag{2}$$

The parameter r_0 determines the radial distance of the virtual surface from the jet axis, which is taken as $r_0 = D$. The coordinate x_0 is used to locate the relative position between the origin of the wave-packet function and the nozzle exit. The two are considered to be coincident in this work, *i.e.*, $x_0 = 0$. The signal growth is controlled by the parameters b_1 and p_1, while b_2 and p_2 define its decaying rate. Following Morris [36], and Papamoschou [22], the solution in the linear regime (*i.e.*, solution for the 3D wave equation in cylindrical polar coordinates) for an arbitrary radial distance $r \geq r_0$ can be evaluated as

$$\begin{aligned} p_w(m, r, x, \theta, t) &= \frac{1}{2\pi} e^{-i\omega t + im\phi} \int_{-\infty}^{\infty} \hat{p}_0(k) \frac{H_m^{(1)}(\lambda r)}{H_m^{(1)}(\lambda r_0)} e^{ikx} dk \\ \text{with} \quad \lambda &= \left[\left(\frac{\omega}{c_\infty}\right)^2 - k^2\right]^{1/2}, \qquad -\frac{\pi}{2} < arg(\lambda) < \frac{\pi}{2}, \end{aligned} \tag{3}$$

where $\hat{p}_0(k)$ is the Fourier transform of $p_0(x)$, c_∞ is the speed of sound of the unperturbed flow, and $H_m^{(1)}$ is the Hankel function of the first kind and order m. In the radiation process, particular care must be taken to the spatial length of the wave-packet from the numerical point of view. A premature truncation of the waveform introduces noise and errors in the signal propagated to higher r. The phase speed can be used to distinguish among the radiative and decaying components of the pressure field generated by the wave-packet, identified respectively by supersonic ($|\omega/k| \geq c_\infty$) and subsonic ($|\omega/k| < c_\infty$) values.

In this work, the method described in Palma *et. al.* [33, 34] is followed and further extended. A wave-packet describing the pressure fluctuations by a free jet is obtained by optimizing its parameters from near-field data on co-axial lines at several radial distances from the jet axis, namely $r/D = 0.5, 1, 2$ and 2.5, and on a far-field polar arc, $r/D = 75$. The reference data used for training the model are obtained through LES simulations[40–42]. A multi-objective optimization procedure aims at matching the complete pressure fluctuation envelope from the model with the one from the numerical simulations for each of the considered lines. The wave-packet obtained is then used as an acoustic source in a Boundary Element formulation to evaluate scattering and reflection from surfaces, *i.e.* installed jet noise.

A. Wave-packet optimization

The wave-packet noise source introduces some parameters whose value can be adjusted to match the actual pressure fluctuation from a reference jet. In this work, this is performed involving a multi-objective optimization procedure. A

generic unconstrained optimization problem consists of the research of the set of variables $\mathbf{v}$ that yields a minimum of the N_J objective functions: $J_n(\mathbf{v}, \mathbf{q})$

$$\begin{aligned} &\text{minimize/maximize } [J_n(\mathbf{v}, \mathbf{q})], \qquad n = 1, ..., N_J \text{ and } \mathbf{v} \in \mathcal{D}_\mathbf{v} \\ &\text{with bounds } v_m^L \leq v_m \leq v_m^U, \qquad m = 1, ..., N_v \end{aligned} \tag{4}$$

where $\mathbf{q}$ is the vector of the parameters, $\mathbf{v}$ is the vector of the N_v design variables bounded by v_n^L and v_n^U in the design space $\mathcal{D}_\mathbf{v}$, In the present application, $\mathbf{v}$ represents the vector collecting the wave-packet parameters $\mathbf{v} = \left[p_1, b_1, p_2, b_2, \omega/(\alpha U_j)\right]$. The number of objective functions to be minimized at the same time is $N_j = 5$, four refer to the near field and one to the far field prediction, described by

$$J_n(\mathbf{x}, \mathbf{y}) = \sqrt{\int_{\mathcal{L}_n} \left(\frac{|p_n - \hat{p}_{LES_n}|}{\max\left(|\hat{p}_{LES_n}|\right)} \right)^2 ds} \tag{5}$$

where $\hat{p}_{LES_n} = p_{LES_n}/\hat{p}$ is the value of the reference pressure field on the n-th line normalized with the maximum value at the line closest to the jet axis $r/D = 0.5$. The objective functions represent the L2-norm of the difference between the pressure predicted by the wave-packet source model and the reference pressure from the LES. The integral is defined over the axial extension, from 0 up to $x/D = 20$, of lines having a constant r_n for the four radial distances in the near field, ($r_1 = 0.5D, D, 2D, 2.5D$), defining $J_1 - J_4$, and over a polar arc, ranging from 15 to 165 degrees, centered on the jet axis at the nozzle exit with radius $R = 75D$ defining J_5. According to Eq. 5, each objective function is normalized by the peak value from the reference pressure field on the respective line $\mathcal{L}_n$.

III. The Boundary Element formulation

The Boundary Element Method (BEM) is a numerical computational method that solves linear partial differential equations formulated as integral equations. Its application is popular in acoustics for the solution of scattering and diffraction problems, exploiting its efficiency in terms of computational resources for problems with a small surface/volume ratio. The linear acoustics problem is here described by the classic D'Alambert operator applied to the pressure p, which in the Laplace domain reads:

$$\nabla^2 p(\mathbf{x}) + \kappa^2 p(\mathbf{x}) = \tilde{q}, \qquad (\mathbf{x}) \in \mathcal{V} \tag{6}$$

where the $\tilde{\bullet}$ indicates Laplace transformation, whereas $\tilde{q}$ represents the acoustics sources present in the domain $\mathcal{V}$, and $\kappa = s/c_0$ is the complex wave number, being $s = \alpha + j\,\omega$ the Laplace variable, and c_0 the speed of sound in the reference conditions. The formulation of the problem in the Laplace domain is equivalent to the time convention $e^{j\,\omega t}$. For this study, we employed an open-source solver AcouSTO [43] for the corresponding Kirchhoff-Helmholtz Integral Equation (KHIE)

$$E(\mathbf{y})\tilde{p}(\mathbf{y}) = \oint_\mathcal{S} \left(G_0 \frac{\partial \tilde{p}}{\partial n} - \tilde{p} \frac{\partial G_0}{\partial n} + s\tilde{p} G_0 \frac{\partial \theta}{\partial n} \right) e^{-s\theta} d\mathcal{S}(\mathbf{x}) + \int_\mathcal{V} G_0 \tilde{q} e^{-s\theta} d\mathcal{V}(\mathbf{x}) \tag{7}$$

where $\mathcal{S} = \partial V$, $s = \alpha + i\omega$ is the Laplace variable, $E(\mathbf{y})$ is the domain function (equal to 1, 1/2, or 0, if $\mathbf{y} \in V$, $\mathbf{y} \in \partial V$, or $\mathbf{y} \notin V$, respectively), and G is the free-field fundamental solution for the 3D KHIE equation defined as

$$G(\mathbf{x}, \mathbf{y}, s) = -\frac{e^{-s\theta}}{4\pi r} = G_0 e^{-s\theta}, \qquad \text{with } r = ||\mathbf{x} - \mathbf{y}|| \quad \text{and } \theta = \frac{r}{c_0} \tag{8}$$

The integral form of the problem is derived directly from the non–homogeneous wave equation, and the acoustic potential $\tilde{p}$ in Eq.7 is the total field, that includes the incident acoustic field and the part scattered by the surfaces $\tilde{p} = \tilde{p}_{in} + \tilde{p}_{sc}$. This formulation is convenient when the primary field produced by the acoustic source in the field is easily calculable. The boundary conditions at the scattering surfaces are given in terms of normal velocity, imposed to be null modeling a rigid boundary

$$\frac{\partial \tilde{p}(\mathbf{x}, \kappa)}{\partial n} = 0. \tag{9}$$

The boundary of the domain is partitioned into N (quadrilateral) panels, and all the quantities are considered to be constant within each panel (0^{th}–order approximation). The collocation method is used by locating the collocation points

at the centers of the panels and the discrete version of Eq.7 is obtained leading to a linear system of equations that reads

$$E\tilde{p}_n = \sum_{m=1}^{N} \left[B_{n,m}\chi_m + \left(C_{n,m} + sD_{n,m}\right)\tilde{p}_m \right] e^{-s\theta_{n,m}} + \tilde{p}_n^I, \qquad n = 1, N \tag{10}$$

where p_n^I is the value of the incident field induced by the sources at the collocation points, and the integral coefficients have the form

$$B_{n,m} = \int_{\mathcal{S}_m} G_0 d\mathcal{S}, \qquad C_{n,m} = \int_{\mathcal{S}_m} \frac{\partial G_0}{\partial n} d\mathcal{S}, \qquad D_{n,m} = \int_{\mathcal{S}_m} G_0 \frac{\partial \theta}{\partial n} d\mathcal{S} \tag{11}$$

The open-source software has been adapted to accept an external custom incident field as input, which in this study is given by Eq. 3. Once the solution is known on the scattering surfaces, Eq. 7 can be used as a boundary integral representation to obtain the solution at arbitrary points in the field.

IV. Numerical database details

The near-field of the isothermal round free jet at a Reynolds number $Re_D = 10^5$ used for this paper has been computed by (LES). The nozzle exhaust jet Mach number has been fixed at $M = 0.9$, with the nozzle-exhaust boundary-layer thickness set at $\delta_{bl} = 0.15r_0$ and the nozzle exit turbulence intensity at 9% (see [41] for details). The LES has been carried out using an in-house solver of the three-dimensional filtered compressible Navier-Stokes equations in cylindrical coordinates (r, θ, x) based on low-dissipation and low-dispersion explicit schemes. The quality of the grid for the present jet LES has been assessed in a previous work [44]. Specifically, the grid contains approximately one billion points. Pressure has been recorded at several locations spanning a large near-field domain and gaining time-resolved signals, see reference [45] for a description of the available data. In addition, the near-pressure field of this jet has been also investigated in [46]. It has been propagated to the far field in [41, 47] using an in-house OpenMP-based solver of the isentropic linearized Euler equations in cylindrical coordinates based on the same numerical methods as the LES. Concerning the near-field domain, we consider arrays of virtual microphones parallel to the nozzle exhaust, containing 1024 probes covering a domain that spans between x=0 and x/D=20. The data have been stored at a sampling frequency corresponding to $St_D = 12.8$, with a total of 3221 time snapshots. A representative one is shown in Fig.1. In the far field, we consider a polar arc of virtual microphones centred at the nozzle exit, positioned at $R = 75D$, from 15 to 165 degrees relative to the jet direction, with a spacing of one degree.

The original pressure signals are represented in terms of their azimuthal components through the azimuthal decomposition [48]. The Fourier coefficients are stored for the first four azimuthal modes that dominate the sound field for low polar angles. As aforementioned the wave-packet model presented in this paper has been carried out for the 0^{th} azimuthal mode, which is dominant for the noise generation at Strouhal numbers lower than 1 [49].

V. Results

A. Wave-packet optimization on free jet

The multi-objective optimization of the wave-packet produces a set of Pareto-efficient solutions constituting the Pareto front, which is a $N_J - 1$ variety in the N_J dimensional codomain. The solutions lying on the front have equal dignity and are optimal in a Paretian sense, *i.e.*, it is not possible, moving along the front, to improve the value of one of the objectives without worsening at least one of the other. One of the techniques that may be employed to identify the preferred solution among the optima is to identify a ranking criterion (also called Decision Maker algorithm). The criterion can be interpreted as an additional objective, allowing the sorting of the solutions on the basis of their score over it and then selecting the solution resulting as the most suitable. Any selection criterion is valid in principle and may be used reasonably, from simple subjective preferences to more complex analyses of the results.

In the present work, the optimal solutions have been sorted by their performance in reproducing the reference field on the far field line. A subset of the Pareto front satisfying $J_5 \leq 2\min(J_5)$ is isolated, and the solution in this subset closest to the utopia point is taken as the preferred one. The parameters of the selected wave-packet are reported in Tab. 1. Figure 2 compares the predicted wave-packet envelopes with the original LES data at different radial distances from the jet axis and at $75D$ from the nozzle exit. Specifically, black continuous lines represent the original data, whilst the optimized wave-packets are in blue dashed lines.

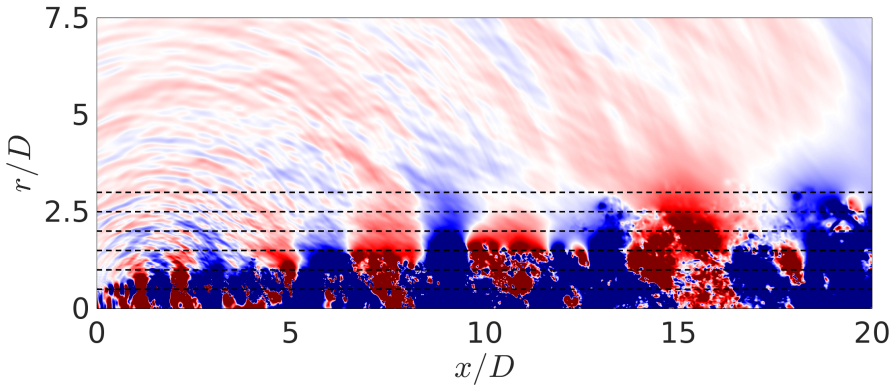

Fig. 1 Snapshot in the (x,r) plane of the pressure signals. The black dashed lines represent the probe arrays in the near field.

Results are presented at this early stage research only for a single St_D number. A value of $St_D = 0.25$ was chosen because it corresponds to the peak Strouhal number in the jet far-field in the downstream direction. Reference data refers to the 0^{th} axisimmetric azimuthal mode, which is predominant in the far-field for the selected St_D. The model predictions are observed to provide a quite good reconstruction of the original data. The directivity is quite well captured in the far-field for almost all the polar angles, Fig. 2f.

B. Scattering prediction

The pressure field produced by the wave-packet source represents the incident field for the scattering calculations by the BEM solver. A simple geometry, sketched in Fig. 3, has been tested to provide a preliminary characterisation of the scattered far-field noise using the BEM method. Specifically, a wedge-shaped flat plate is used as a scattering body, representing a wing interacting with the pressure perturbation emitted by the jet. The wing has been extended upstream to minimise the scattering from the leading edge and has been designed sufficiently large in a spanwise direction to avoid side edge effects. The wave-packet frame of reference is fixed on the symmetry plane of the wing, at $\Delta x_p = D$ from the plate leading edge and $\Delta z_p = D$ in the radial direction. The flat plate extends for $l_p = 4D$ in the x (jet-axis) direction, and its span is $s_p = 10D$.

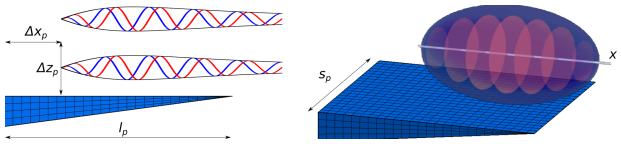

Fig. 3 Sketch of the BEM setup

The far-field pressure field is presented in Fig 4 comparing installed and isolated jet configurations. It is worth noting that a substantial noise increase has been predicted at higher polar angles in the installed case, according to the literature [30]. This indicates that the model is able to capture quite well the jet-wing scattering noise. However, further analyses are needed to include different St_D numbers in the analysis, increasing the robustness of the model.

VI. Conclusions

A multi-objective optimization of a wave-packet, including both near- and far-field noise, is presented to predict the behaviour of the 0^{th} azimuthal mode. A Pareto front has been obtained as a solution for the optimization due to the

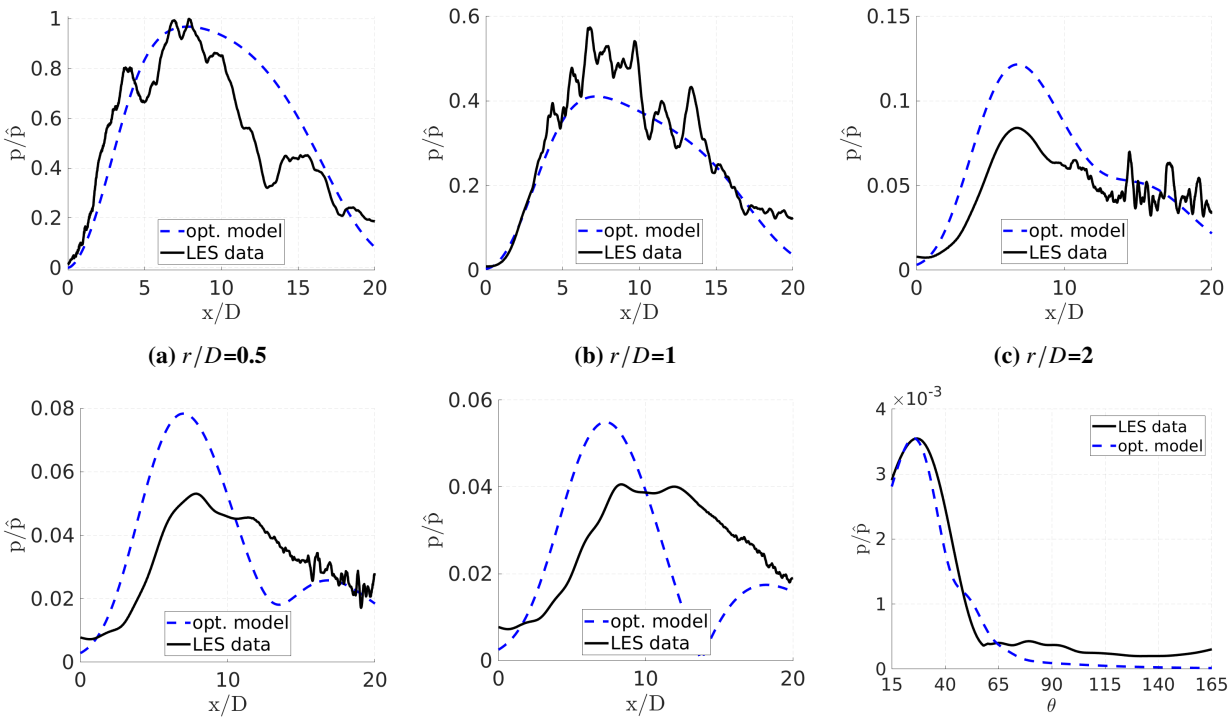

(a) r/D**=0.5** **(b)** r/D**=1** **(c)** r/D**=2**

(d) r/D**=2.5** **(e)** r/D**=3** **(f)** R**=75D**

Fig. 2 Comparison between reference and optimized wave-packet normalized pressure. Near-field predictions in Figures from (a) to (e), far-field prediction in (f), $St_D = 0.25$**.**

St_D	p_1	b_1	p_2	b_2	$\omega/(\alpha U_j)$
0.25	1.7190	0.0983	4.5929	0.3985	0.8768

Table 1 Wave-packet parameters

concurrency between the different objectives. The preferred solution on the front is then selected using a Pareto ranking criterion method, considering the performance of the solution in reproducing both the near- and the far-field reference pressure field. The results of the optimizations are found to provide a good agreement between the reference numerical data, generated through well-resolved LES simulations, and the model in the tested Strouhal number ($St_D = 0.25$).

The optimized wave-packet has been coupled with a BEM solver to predict the installation effects in terms of scattering noise. The noise increase in the upstream scattered field of the installed configuration shows the adherence of the simulations to the physics observed experimentally.

Further investigations that will involve multi-Strouhal analyses, including the possibility of reducing the use of flow-immersed virtual probes, which can be a limit of the model, are currently ongoing. The opportunity to use different objective functions and wave-packet shapes will also be explored.

References

[1] Baudin, C., Lefèvre, M., Champelovier, P., Lambert, J., Laumon, B., and Evrard, A.-S., "Aircraft Noise and Psychological Ill-Health: The Results of a Cross-Sectional Study in France," *Int J Environ Res Public Health*, Vol. 15, No. 8, 2018.

[2] Basner, M., and McGuire, S., "WHO Environmental Noise Guidelines for the European Region: A Systematic Review on Environmental Noise and Effects on Sleep," *Int J Environ Res Public Health*, Vol. 15, No. 3, 2018.

[3] Burghignoli, L., Di Marco, A., Centracchio, F., Camussi, R., Ahlefeldt, T., Henning, A., Adden, S., and Di Giulio, M.,

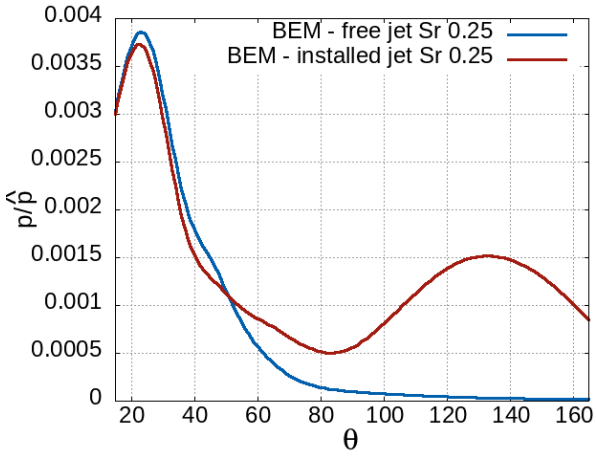

Fig. 4 Comparison between isolated and installed jet far-field acoustic pressures at $St = 0.25$ from BEM simulations.

"Evaluation of the noise impact of flap-tip fences installed on laminar wings," *CEAS Aeronautical Journal*, Vol. 11, No. 4, 2020, pp. 849–872. https://doi.org/10.1007/s13272-020-00454-x.

[4] Jawahar, H. K., Meloni, S., and Camussi, R., "Jet noise sources for chevron nozzles in under-expanded condition," *International Journal of Aeroacoustics*, Vol. 0, No. 0, 0, p. 1475472X221101766. https://doi.org/10.1177/1475472X221101766.

[5] Meloni, S., and Kamliya Jawahar, H., "A Wavelet-Based Time-Frequency Analysis on the Supersonic Jet Noise Features with Chevrons," *Fluids*, Vol. 7, No. 3, 2022, p. 108.

[6] Iemma, U., and Palma, G., "Optimization of metasurfaces for the design of noise trapping metadevices," *Proceedings of the 26th International Congress on Sound and Vibration, ICSV 2019*, 2019.

[7] Palma, G., and Burghignoli, L., "On the integration of acoustic phase-gradient metasurfaces in aeronautics," *International Journal of Aeroacoustics*, Vol. 19, No. 6-8, 2020, pp. 294–309. https://doi.org/10.1177/1475472x20954404.

[8] Palma, G., Burghignoli, L., Centracchio, F., and Iemma, U., "Innovative Acoustic Treatments of Nacelle Intakes Based on Optimised Metamaterials," *Aerospace*, Vol. 8, No. 10, 2021. https://doi.org/10.3390/aerospace8100296.

[9] Jones, M. G., Nark, D. M., and Schiller, N. H., *Evaluation of Variable-Depth Liners with Slotted Cores*, 2022. https://doi.org/10.2514/6.2022-2823.

[10] Dodge, C., Howerton, B. M., and Jones, M. G., *An Acoustic Liner with a Multilayered Active Facesheet*, 2022. https://doi.org/10.2514/6.2022-2902.

[11] Palani, S., Murray, P., McAlpine, A., Knepper, K., and Richter, C., *Experimental and numerical assessment of novel acoustic liners for aero-engine applications*, 2022. https://doi.org/10.2514/6.2022-2900.

[12] Palma, G., Centracchio, F., and Burghignoli, L., "Optimized metamaterials for enhanced noise shielding of innovative aircraft configurations," *Proceedings of the 27th International Congress on Sound and Vibration, ICSV 2021*, 2021.

[13] Liebeck, R. H., "Design of the Blended Wing Body Subsonic Transport," *Journal of Aircraft*, Vol. 41, No. 1, 2004, pp. 10–25. https://doi.org/10.2514/1.9084.

[14] Centracchio, F., Burghignoli, L., Rossetti, M., and Iemma, U., "Noise shielding models for the conceptual design of unconventional aircraft," *INTER-NOISE 2018 - 47th International Congress and Exposition on Noise Control Engineering: Impact of Noise Control Engineering*, 2018.

[15] Burghignoli, L., Centracchio, F., Iemma, U., and Rossetti, M., "Multi-objective optimization of BWB aircraft for noise shielding improvement," *25th International Congress on Sound and Vibration 2018, ICSV 2018: Hiroshima Calling*, Vol. 2, 2018, p. 1256 – 1263.

[16] Xie, J., Cai, Y., Chen, M., and Mavris, D. N., *Integrated Sizing and Optimization of Hybrid Wing Body Aircraft in Conceptual Design*, 2019. https://doi.org/10.2514/6.2019-2885.

[17] Papamoschou, D., and Mayoral, S., "Jet noise shielding for advanced hybrid wing-body configuration," *49th AIAA Aerospace Sciences Meeting including the New Horizons Forum and Aerospace Exposition*, 2011, p. 912.

[18] Denisov, S., and Korolkov, A., "Investigation of noise-shielding efficiency with the method of sequences of maximum length in application to the problems of aviation acoustics," *Acoustical Physics*, Vol. 63, No. 4, 2017, pp. 462–477.

[19] Burghignoli, L., Rossetti, M., Centracchio, F., Palma, G., and Iemma, U., "Adaptive RBF with hyperparameter optimisation for aeroacoustic applications," *International Journal of Aeroacoustics*, Vol. 21, No. 1-2, 2022, pp. 22–42. https://doi.org/10.1177/1475472X221079545.

[20] Centracchio, F., Burghignoli, L., Palma, G., Cioffi, I., and Iemma, U., "Noise shielding surrogate models using dynamic artificial neural networks," *INTER-NOISE and NOISE-CON Congress and Conference Proceedings*, Vol. 263, No. 1, 2021, pp. 5216–5224. https://doi.org/10.3397/in-2021-3008.

[21] Centracchio, F., Meloni, S., Jawahar, H. K., Azarpeyvand, M., Camussi, R., and Iemma, U., *Under-expanded jet noise prediction using surrogate models based on artificial neural networks*, 2022. https://doi.org/10.2514/6.2022-3025.

[22] Papamoschou, D., *Prediction of Jet Noise Shielding*, 2010. https://doi.org/10.2514/6.2010-653.

[23] Kopiev, V. F., and Chernyshev, S. A., "Simulation of azimuthal characteristics of turbulent jet noise by correlation model of quadrupole noise sources," *International Journal of Aeroacoustics*, Vol. 13, No. 1-2, 2014, pp. 39–60.

[24] Denisov, S., Kopiev, V., Ostrikov, N., Faranosov, G., and Chernyshev, S., "Using the Correlation Model of Random Quadrupoles of Sources to Calculate the Efficiency of Turbulent Jet Noise Screening with Geometric Diffraction Theory," *Acoustical Physics*, Vol. 66, No. 5, 2020, pp. 528–541.

[25] Jordan, P., and Colonius, T., "Wave Packets and Turbulent Jet Noise," *Annual Review of Fluid Mechanics*, Vol. 45, No. 1, 2013, pp. 173–195. https://doi.org/10.1146/annurev-fluid-011212-140756.

[26] Kœnig, M., Cavalieri, A. V., Jordan, P., Delville, J., Gervais, Y., and Papamoschou, D., "Farfield filtering and source imaging of subsonic jet noise," *Journal of Sound and Vibration*, Vol. 332, No. 18, 2013, pp. 4067–4088. https://doi.org/doi.org/10.2514/6.2010-3779.

[27] Huang, C., and Papamoschou, D., *Numerical Study of Noise Shielding by Airframe Structures*, 2008. https://doi.org/10.2514/6.2008-2999.

[28] Papamoschou, D., *Wavepacket Modeling of the Jet Noise Source*, 2011. https://doi.org/10.2514/6.2011-2835.

[29] Papamoschou, D., "Wavepacket modeling of the jet noise source," *International Journal of Aeroacoustics*, Vol. 17, No. 1-2, 2018, pp. 52–69. https://doi.org/10.1177/1475472X17743653.

[30] Meloni, S., Proença, A. R., Lawrence, J. L., and Camussi, R., "An experimental investigation into model-scale installed jet–pylon–wing noise," *Journal of Fluid Mechanics*, Vol. 929, 2021. https://doi.org/10.1017/jfm.2021.831.

[31] Meloni, S., Mancinelli, M., Camussi, R., and Huber, J., "Wall-Pressure Fluctuations Induced by a Compressible Jet in Installed Configuration," *AIAA Journal*, Vol. 58, No. 7, 2020, pp. 2991–3000. https://doi.org/10.2514/1.J058791.

[32] Jordan, P., Jaunet, V., Towne, A., Cavalieri, A. V. G., Colonius, T., Schmidt, O., and Agarwal, A., "Jet–flap interaction tones," *Journal of Fluid Mechanics*, Vol. 853, 2018, p. 333–358. https://doi.org/10.1017/jfm.2018.566.

[33] Palma, G., Meloni, S., Camussi, R., Iemma, U., and Bogey, C., *A Multi-Objective Optimization of a Wave-Packet Model Using Near-Field Subsonic Jet Data*, 2022. https://doi.org/10.2514/6.2022-2934.

[34] Palma, G., Meloni, S., Camussi, R., Iemma, U., and Bogey, C., "Data-Driven Multiobjective Optimization of Wave-Packets for Near-Field Subsonic Jet Noise," *AIAA Journal*, Vol. 61, No. 5, 2023, pp. 2179–2188. https://doi.org/10.2514/1.J062261.

[35] Morris, P. J., "Jet noise prediction: Past, present and future," *Canadian Acoustics*, Vol. 35, No. 3, 2007, p. 16–22.

[36] Morris, P. J., "A Note on Noise Generation by Large Scale Turbulent Structures in Subsonic and Supersonic Jets," *International Journal of Aeroacoustics*, Vol. 8, No. 4, 2009, pp. 301–315. https://doi.org/10.1260/147547209787548921.

[37] Tam, C. K. W., and Burton, D. E., "Sound generated by instability waves of supersonic flows. Part 2. Axisymmetric jets," *Journal of Fluid Mechanics*, Vol. 138, 1984, p. 273–295. https://doi.org/10.1017/S0022112084000124.

[38] Crighton, D. G., and Huerre, P., "Shear-layer pressure fluctuations and superdirective acoustic sources," *Journal of Fluid Mechanics*, Vol. 220, 1990, p. 355–368. https://doi.org/10.1017/S0022112090003299.

[39] Avital, E. J., Sandham, N. D., and Luo, K. H., "Mach Wave Radiation by Mixing Layers. Part I: Analysis of the Sound Field," *Theoretical and Computational Fluid Dynamics*, Vol. 12, 1998, pp. 73–90. https://doi.org/doi.org/10.1007/s001620050100.

[40] Bogey, C., Marsden, O., and Bailly, C., "Large-eddy simulation of the flow and acoustic fields of a Reynolds number 105 subsonic jet with tripped exit boundary layers," *Physics of Fluids*, Vol. 23, 2011, p. 035104. https://doi.org/doi.org/10.1063/1.3555634.

[41] Bogey, C., "Acoustic tones in the near-nozzle region of jets: characteristics and variations between Mach numbers 0.5 and 2," *Journal of Fluid Mechanics*, Vol. 921, 2021, p. A3. https://doi.org/10.1017/jfm.2021.426.

[42] Camussi, R., Meloni, S., and Bogey, C., "On the influence of the nozzle exhaust initial conditions on the near field acoustic pressure," *Acta Acustica*, Vol. 6, 2022, p. 57.

[43] Palma, G., Burghignoli, L., Marchese, V., and Iemma, U., "Implementation of a dual surface regularization technique in ACA-based BEM solver," *Proceedings of the 28th International Congress on Sound and Vibration, ICSV 2022*, 2022.

[44] Bogey, C., "Grid sensitivity of flow field and noise of high-Reynolds-number jets computed by large-eddy simulation," *International Journal of Aeroacoustics*, Vol. 17, 2018, pp. 399 – 424. https://doi.org/doi.org/10.1177/1475472X18778287.

[45] Bogey, C., "A database of flow and near pressure field signals obtained for subsonic and nearly ideally expanded supersonic free jets using large-eddy simulations," https://hal.archives-ouvertes.fr/hal-03626787, 2022.

[46] Adam, A., Papamoschou, D., and Bogey, C., "Imprint of Vortical Structures on the Near-Field Pressure of a Turbulent Jet," *AIAA Journal*, Vol. 60, No. 3, 2022, pp. 1578–1591. https://doi.org/10.2514/1.J061010.

[47] Bogey, C., "Tones in the acoustic far field of jets in the upstream direction," *AIAA J.*, Vol. 60, No. 4, 2022, pp. 2397–2406. https://doi.org/10.2514/1.J061013.

[48] Michalke, A., and Fuchs, H., "On turbulence and noise of an axisymmetric shear flow," *Journal of Fluid Mechanics*, Vol. 70, No. 1, 1975, pp. 179–205. https://doi.org/10.1017/S0022112075001966.

[49] Cavalieri, A. V. G., Jordan, P., Colonius, T., and Gervais, Y., "Axisymmetric superdirectivity in subsonic jets," *Journal of Fluid Mechanics*, Vol. 704, 2012, p. 388–420. https://doi.org/10.1017/jfm.2012.247.